Two-photon Excited Fluorescence of Nitrogen-Vacancy Centers in Proton-Irradiated Type Ib Diamond[†]

Tse-Luen Wee,[‡,§] Yan-Kai Tzeng,[£] Chau-Chung Han,[‡] Huan-Cheng Chang,[*,‡,£]
Wunshain Fann,[‡] Jui-Hung Hsu,[*,#] Kuan-Ming Chen,[¶] and Yueh-Chung Yu[¶]

Institute of Atomic and Molecular Sciences, Academia Sinica, Taipei 106, Taiwan, Department of Chemistry, National Tsing Hua University, Hsinchu 300, Taiwan, Department of Chemistry, National Taiwan Normal University, Taipei 106, Taiwan, Department of Materials Science and Optoelectronic Engineering, National Sun Yat-Sen University, Kaohsiung 804, Taiwan, and Institute of Physics, Academia Sinica, Taipei 115, Taiwan

Two-photon fluorescence spectroscopy of negatively charged nitrogen-vacancy [(N-V)$^-$] centers in type Ib diamond single crystals have been studied with a picosecond (7.5 ps) mode-locked Nd:YVO$_4$ laser operating at 1064 nm. The (N-V)$^-$ centers were produced by radiation damage of diamond using a 3 MeV proton beam, followed by thermal annealing at 800 °C. Prior to the irradiation treatment, infrared spectroscopy of the C–N vibrational modes at 1344 cm^{-1} suggested a nitrogen content of 109 ± 10 ppm. Irradiation and annealing of the specimen led to the emergence of a new absorption band peaking at ~560 nm. From a measurement of the integrated absorption intensity of the sharp zero-phonon line (637 nm) at liquid nitrogen temperature, we determined a (N-V)$^-$ density of (4.5 ± 1.1) × 10^{18} centers/cm^3 (or 25 ± 6 ppm) for the substrate irradiated at a dose of 1 × 10^{16} H$^+$/cm^2. Such a high defect density allowed us to observe two-photon excited fluorescence and measure the corresponding fluorescence decay time. No significant difference in the spectral feature and fluorescence lifetime was observed between one-photon and two-photon excitations. Assuming that the fluorescence quantum yields are the same for both processes, a two-photon absorption cross section of σ_{TPA} = (0.45 ± 0.23) × 10^{-50} cm^4·s/photon at 1064 nm was determined for the (N-V)$^-$ center based on its one-photon absorption cross section of σ_{OPA} = (3.1 ± 0.8) × 10^{-17} cm^2 at 532 nm. The material is highly photostable and shows no sign of photobleaching even under continuous two-photon excitation at a peak power density of 3 GW/cm^2 for 5 min.

Introduction

Diamonds, prevailing as jewels and industrial grinding materials, find a stage in modern biotechnology.[1–3] The material is biocompatible, nontoxic, chemically inert, and environmentally benign.[4,5] Moreover, the surfaces of nanoscale diamond particles can be easily derivatized with functional groups such as carboxyl and amino moieties.[6,7] They can carry desired biomolecules for applications in targeted delivery and gene therapies. While many other carriers usually require additional labeling with organic dye molecules or fluorescent proteins in order to be probed optically, some specially fabricated nano-diamonds themselves are capable of fluorescing without photobleaching and blinking for facile detection with optical microscopy.[4,8] These fluorescent nanodiamonds (FNDs) bear the common feature of containing nitrogen-vacancy (N-V) defect centers, which can be produced by high-energy electron (or ion) irradiation of type Ib diamond crystallites followed by thermal annealing.[9,10] An experiment on single-particle tracking of FNDs in living cells has been recently demonstrated,[8] highlighting the superb photophysical and biochemical properties of this novel

nanomaterial. A combination of these unique properties including chemical inertness, low cytotoxicity, high fluorescence brightness, absence of photobleaching and blinking, and easiness of surface functionalization endows FND with great attraction to be used as biological fluorescent probes and as drug, protein, and gene carriers.

Of many vacancy-related defect centers in type Ib diamond, (N-V)$^-$ is most noteworthy. The center, carrying a negative charge,[11] is the dominant end product of thermal annealing of radiation-damaged diamond at temperatures above 800 °C.[9,10] It exhibits a sharp zero-phonon line at 637 nm for the ^{3}A → ^{3}E electronic transition,[12] along with a broad phonon sideband peaking at ~560 nm. Its emission occurs at 600–800 nm, a region well suited for biomedical imaging. Our previous studies[8] have shown that one-photon excited fluorescence of the (N-V)$^-$ center can be readily detected at the single-particle level for 35 nm FNDs in biological cells using a confocal fluorescence microscope equipped with a cw 532 nm laser. While the emission has a long penetration depth through biological samples such as tissues and cells,[13] the excitation light does not. Two-photon excitation becomes an obvious choice,[14–16] which offers additional advantages such as point-like excitation, suppression of out-of-focus noises, effective elimination of background scattered light, and so forth. A fundamental understanding of the two-photon absorption and emission processes associated with (N-V)$^-$ is thus desired. The understanding should help us to choose the optimal laser wavelength and relevant experi-

---

* To whom correspondence should be addressed. E-mail: hcchang@po.iams.sinica.edu.tw (H.-C.C.); jhsu@mail.nsysu.edu.tw (J.-H.H.).
[‡] Institute of Atomic and Molecular Sciences, Academia Sinica.
[§] National Tsing Hua University.
[£] National Taiwan Normal University.
[#] National Sun Yat-Sen University.
[¶] Institute of Physics, Academia Sinica.

mental conditions for high-sensitivity monitoring of FNDs in tissues and body fluids with two-photon fluorescence microscopy.

The (N-V)⁻ center in diamond has no center of symmetry, and therefore, its one-photon-allowed transition is not forbidden by selection rules in the two-photon absorption (TPA), which is a third-order nonlinear optical process.[17,18] To delineate the two-photon excited fluorescence properties of this center, knowing the strengths of both TPA and TPE (two-photon emission) is essential. However, because only a small fraction of excitation photons is absorbed in the nonlinear process, direct measurement of the TPA cross section (σ_{TPA}) is difficult. A more feasible approach is to measure the relative strength of TPE to that of OPE (one-photon emission) under identical experimental conditions.[19] Mathematically, the relative emission strength can be expressed as

$$\frac{I_{TPE}}{I_{OPE}} = \frac{A_{TP} \cdot t_{TP} \cdot \sigma_{TPA} \cdot P_{TP}^2 \cdot Q_{TPE}}{A_{OP} \cdot t_{OP} \cdot \sigma_{OPA} \cdot P_{OP} \cdot Q_{OPE}} \qquad (1)$$

where I is the observed fluorescence intensity, A is the excitation area, t is the probed sample thickness, σ is the excitation cross section, P is the excitation power density (or photon irradiance), and Q is the fluorescence quantum yield. For an excitation that relaxes rapidly to the bottom of the potential well of the excited state, it is reasonable to assume that both OPE and TPE have the same fluorescence quantum yields, that is, $Q_{TPE}/Q_{OPE} = 1$. The ratio of the excitation volume (i.e., $A_{TP} \cdot t_{TP}/A_{OP} \cdot t_{OP}$), on the other hand, can be determined by careful calibration of the experimental setup with molecular fluorophores (such as rhodamine B and fluorescein) of known absorption cross sections,[19,20] from which the value of σ_{TPA} can be obtained if the corresponding one-photon absorption cross section (σ_{OPA}) has also been measured experimentally.

This work was aimed to characterize the nonlinear photophysical properties of FNDs produced by proton irradiation. However, due to the high refractive index of diamond, $n = 2.42$,[21] strong scattering of the light from diamond−air interfaces makes it very difficult (if not impossible) to observe even OPA spectra of FNDs. A type Ib diamond single crystal was thus used to facilitate the spectroscopic characterization process. Use of the single crystals has allowed us not only to quantify the concentration of (N-V)⁻ centers created by the proton irradiation but also to assess the efficacy of the irradiation (and subsequent thermal annealing) process with both infrared and UV−visible absorption spectroscopies. The result serves as an important guidance for our future optimization of the fluorescence brightness of FNDs produced with an ion beam in general. By using a picosecond mode-locked Nd:YVO₄ laser operating at 1064 nm as the light source and a high numerical aperture objective to collect two-photon excited fluorescence, we have been able to obtain the TPE spectra of the (N-V)⁻ centers. The associated absorption cross section and fluorescence lifetime were also determined for the first time.

Experimental Section

Synthetic type Ib diamond single crystals of two different crystallographic orientations ([100] and [111]) were obtained from Element Six. They were golden yellow in color and contained typically 100 ppm of nitrogen atoms. The as-received diamond flake (typically 0.8 mm in thickness) was irradiated by a 3 MeV proton beam from a NEC tandem accelerator (9SDH-2, National Electrostatics Corporation) at a dose of 1 × 10¹⁶ H⁺/cm². The typical current of the proton beam was
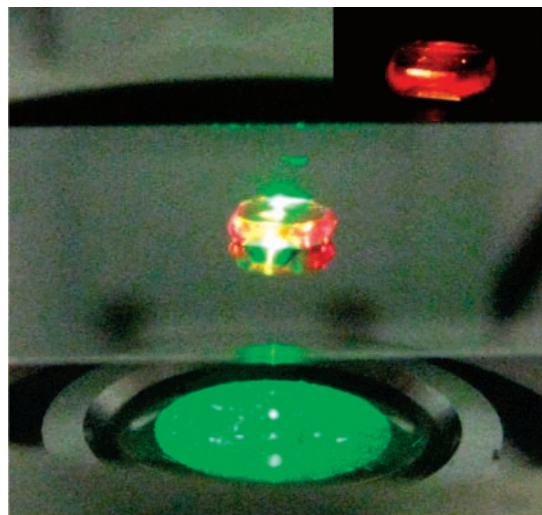

Figure 1. A photo showing the bright-red emission from a proton-irradiated type Ib diamond single crystal illuminated by green light from an inverted fluorescence microscope. The image after filtering out the green scattered light is shown in the upper right corner. The proton beam energy used to create the N-V centers in this sample was 3 MeV.

0.1 μA, with a spatially averaged beam flux of 6 × 10¹¹ protons/cm²·s at the sample target. After ∼5 h of continuous irradiation at room temperature to create vacancies, (N-V)⁻ centers formed upon annealing the sample in vacuum at 800 °C for 2 h in a quartz tube. A UV−vis spectrophotometer (U-3310, Hitachi) operating at an instrumental resolution of 1 nm and a Fourier-transform infrared (FTIR) spectrometer (MB-154, BOMEM) operating at an instrumental resolution of 1 cm⁻¹ characterized the absorption spectra of the diamond substrates before and after the irradiation/annealing treatment. The corresponding fluorescence images were obtained using a laser scanning confocal fluorescence microscope (C-1, Nikon) equipped with a 5 mW 543 nm He−Ne laser and a long-pass filter set for collection of fluorescence at the wavelength of $\lambda > 590$ nm. Both the laser excitation and fluorescence collection were made through a 60× oil-immersion objective with a numerical aperture (NA) of 1.4. A photo showing the bright red emission from a proton-irradiated [100]-oriented diamond crystal illuminated by the green light from the fluorescence microscope is exhibited in Figure 1.

Figure 2 shows an optical layout of the experimental setup used to measure the two-photon fluorescence spectra and decay lifetimes. One-photon excitation experiments were also conducted using the same setup with two manual switches to change optics and guide the desired light beams. The excitation source consisted of a diode-pumped mode-locked Nd:YVO₄ laser (IC-400-ps, High Q Laser), which provided both 532 and 1064 nm light pulses with widths of 7.5 ps at a repetition rate of 50 MHz. The two laser beams were first separated spatially, collimated independently, and then recombined after proper energy attenuation. Depending on the fluorescence intensity, they were focused by either an air objective (40×, NA 0.6) or an oil-immersion objective (100×, NA 1.4) mounted on a piezoelectric nanopositioner (NanoF100, Mad City Laboratory) for fine adjustment. The beam collimation, together with the confocal configuration, ensured good spatial overlap of the two laser beams on the same sample spot. Spectra of both the one-photon and the two-photon excited fluorescence, after passing through two 532 nm Raman filters (538AELP, Omega Optical, and LP03-532RU, Semrock) and an 800 nm short-pass filter (E800SP, Chroma), were acquired using a monochromator
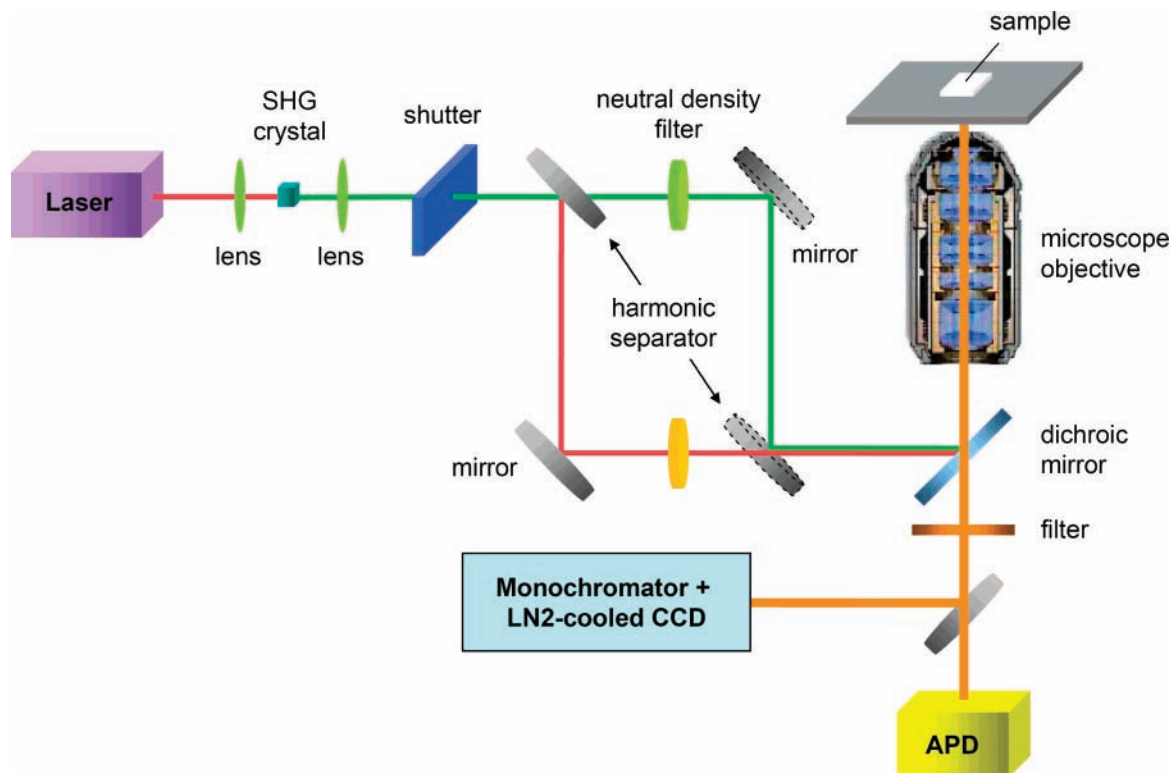
Figure 2. An optical layout of the experimental setup for both one-photon and two-photon excited fluorescence measurements using a 7.5 ps Nd:YVO₄ laser. See text for further details.

(SP500i, Acton Research) equipped with a liquid-nitrogen-cooled CCD camera (LN/CCD-Spec10-100B, Princeton Instruments). To measure the fluorescence intensities and associated decay lifetimes, the emission was detected with an APD (avalanche photodiode) single-photon counting module (SPCM-AQR-14-FC, Perkin-Elmer) or a time-correlated single-photon counting module (SPC-830, Becker and Hickl) at an interval of 4.8 ps/channel. The typical average laser power used in the OPE and TPE measurements was 0.2 μW and 40 mW, respectively.

An essence of using the proton beam to produce (N-V)⁻ centers in diamond is to lower the ion energy to a level of less than 100 keV so that production of FNDs can be carried out routinely and safely in general research laboratories. However, concerns with the efficacy of the medium-energy ion irradiation exist.[22] To test the applicability of this method, a preliminary experiment using a 40 keV ion beam was conducted. The beam, without any mass discrimination, was composed of ∼95% H⁺ and ∼5% H₃⁺. It was generated by discharge of pure H₂ in a positive rf ion source (National Electrostatics Corporation) and guided by a high-voltage acceleration tube in a vacuum chamber (base pressure ∼ 2 × 10⁻⁷ Torr) built in house. The output current of the unfocused proton beam emanating from this ion source was constantly ∼100 μA, which was nearly 3 orders of magnitude higher than that of the 3 MeV protons. The spatially averaged beam flux at the target sample was ∼6 × 10¹³ H⁺/cm²·s. The typical irradiation dose used in this experiment was 6 × 10¹⁴ H⁺/cm².

Results and Discussion

Proton Beam Irradiation and Penetration Depth. Conventionally, the (N-V)⁻ centers in diamond were produced via bombardment of the sample with high-energy (typically 2 MeV) electrons generated from a van der Graaff accelerator, followed by thermal annealing at elevated temperatures (typically 800

°C).[9,10] The requirement for such highly specialized equipment prevents the possibility of mass production of FNDs. A beam of low-mass ions (such as H⁺ and He⁺) is a promising alternative since the threshold energy of the radiation damage by these ions is lower than 1 keV, in contrast to the corresponding 180 keV for the electron.[23,24] According to the SRIM Monte Carlo simulations,[25] a 3 MeV proton beam incident along the [100] direction can penetrate diamond with a depth of 50 μm (Figure 3a), assuming a displacement energy of 37.5 eV for the carbon atoms.[24] The penetration depth reduces to 0.23 μm at the beam energy of 40 keV (Figure 3b), and the number of vacancies created per proton decreases from 13 to 4, accordingly.[26] We have previously demonstrated that bright FNDs can indeed be produced by the 3 MeV proton irradiation.[4] For type Ib diamond crystallites as an example, exposure of the specimen to the 3 MeV protons at a dose of 1 × 10¹⁶ H⁺/cm² is expected to produce (N-V)⁻ centers (after thermal annealing) with a concentration in the range of ∼1 × 10⁷ centers/μm³, assuming little vacancy annihilation,[27] divacancy formation, and irradiation overdose.[28] This high defect concentration alternatively suggests that each 10 nm diamond particle can contain up to 10 (N-V)⁻ centers in its crystal lattice. These particles are anticipated to have a fluorescence brightness comparable to that of semiconductor quantum dots such as CdTe emitting light in the similar wavelength region (i.e., 700 nm).

To understand how protons interact with diamond, one of the previous studies[29,30] used Raman spectroscopy to probe the crystalline integrity of diamond substrates damaged by 600 keV protons. In that study,[30] the specimen was analyzed without thermal annealing in order to observe the resulting microstructural changes based on the Raman signatures pertinent to graphitic carbons. The authors demonstrated that SRIM can accurately predict the maximal penetration depth of the proton within an error of ∼1 μm out of 5 μm. Figure 4a shows a side view of the diamond substrate prepared in this work with the 3
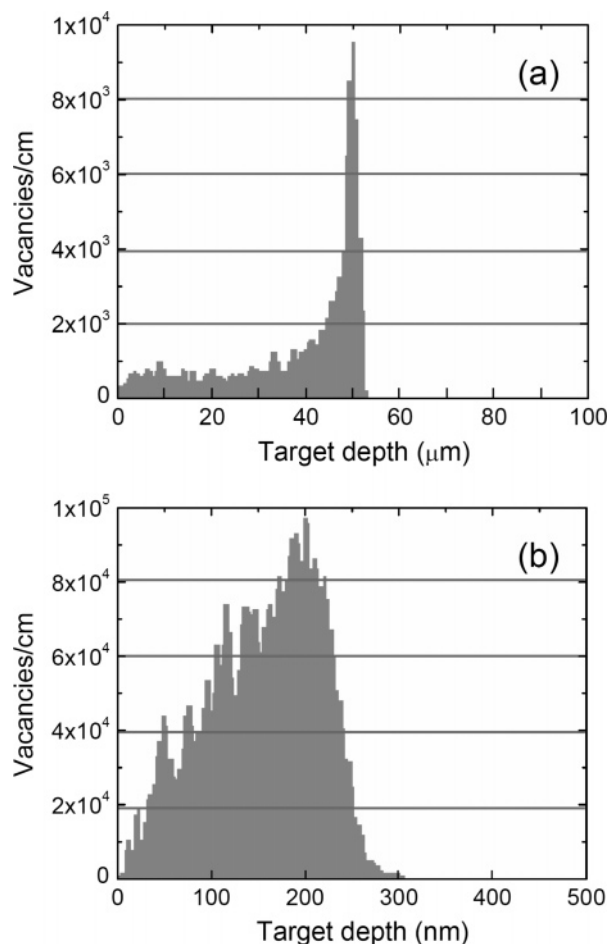
Figure 3. Spatial distribution of vacancies produced in diamond as a function of target depth at a proton irradiation energy of (a) 3 MeV and (b) 40 keV as predicted by SRIM Monte Carlo simulations. The number of damage events used in both simulations is 9999.

MeV proton irradiation followed by 800 °C annealing. A dark, reddish band can be clearly identified near the substrate's front surface (i.e., the *xy* plane in the figure). It has a thickness of 50 μm, in very good agreement with the range of the vacancy production predicted by the SRIM simulation (Figure 3a). The corresponding fluorescence image, on the other hand, can be obtained by using laser scanning confocal fluorescence micros-copy. Operating the fluorescence microscope in the confocal mode allowed us to map out the (N-V)$^-$ distribution profile as a function of the target sample depth (i.e., the *z* axis) with a spatial resolution of $\sim$300 nm.[31] Shown in Figure 4b is a two-dimensional scan of the specimen in the *xz* plane. As seen, the fluorescence spreads over a distance of $\sim$50 μm along the *z* axis near the air−diamond interface ($z = 0$). Since the fluorescence was collected at the diamond edge, whose surface is corrugated and fractured, the image obtained here is very likely distorted due to the large refractive index difference between diamond and air. Therefore, the observed intensity profile as given in Figure 4c may not represent the true distribution of the (N-V)$^-$ centers in the crystal lattice. Nevertheless, there is an evident drop of the fluorescence intensity to the background level in the profile at $z \approx 50$ μm. The result is in good accord with the observation of a clear border that separates regions with and without proton irradiation at $z \approx 50$ μm in Figure 4a.

For samples prepared with the 40 keV protons, the vacancy-associated visible absorption band is too thin to be identified in the bright-field image (Figure 5a). Applying the confocal
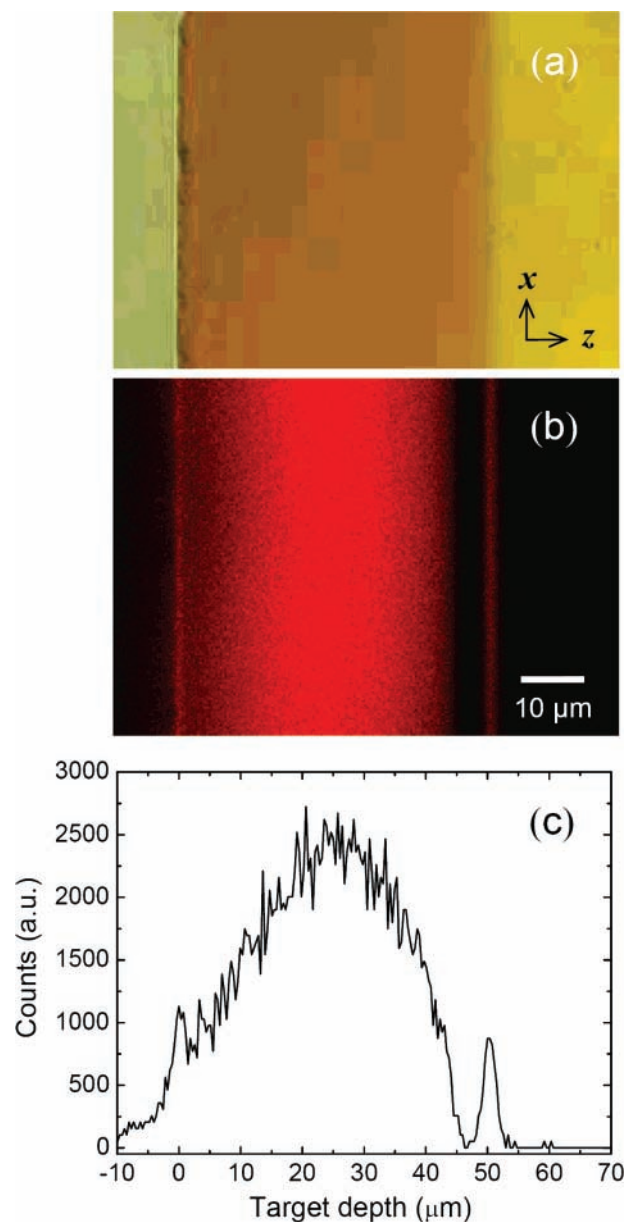

Figure 4. Characterization of a diamond substrate irradiated by 3 MeV protons and annealed at 800 °C with confocal fluorescence microscopy; (a) bright field and (b) confocal fluorescence images of the substrate near one of its surface edges. A typical fluorescence intensity profile along the *z* axis is shown in (c).

imaging technique, however, reveals a dim and irregular red emission layer near the air−diamond interface (Figure 5b). The layer has a thickness of 630 nm, most probably limited by the resolution of the confocal fluorescence microscope scanning along the rough edge surface. A comparison of the fluorescence intensities between Figures 4c and 5c suggests that the concentration of the N-V centers created by the 40 keV protons is about a factor of 2 lower than that produced by the 3 MeV photons. Overall, the enhancement of the fluorescence intensity due to the proton irradiation and thermal annealing treatment is more than 4 orders of magnitude.

N-V Concentration and OPA Cross Section. One of the advantages of using diamond single crystals in this experiment is that it allows observation of the infrared spectra of C−N vibrations and the OPA spectra of the $^3A \rightarrow \, ^3E$ electronic transition of the (N-V)$^-$ center. Thanks to the increased accuracy in the calibrations that link the concentrations of vacancy-related centers with the strengths of their characteristic absorption
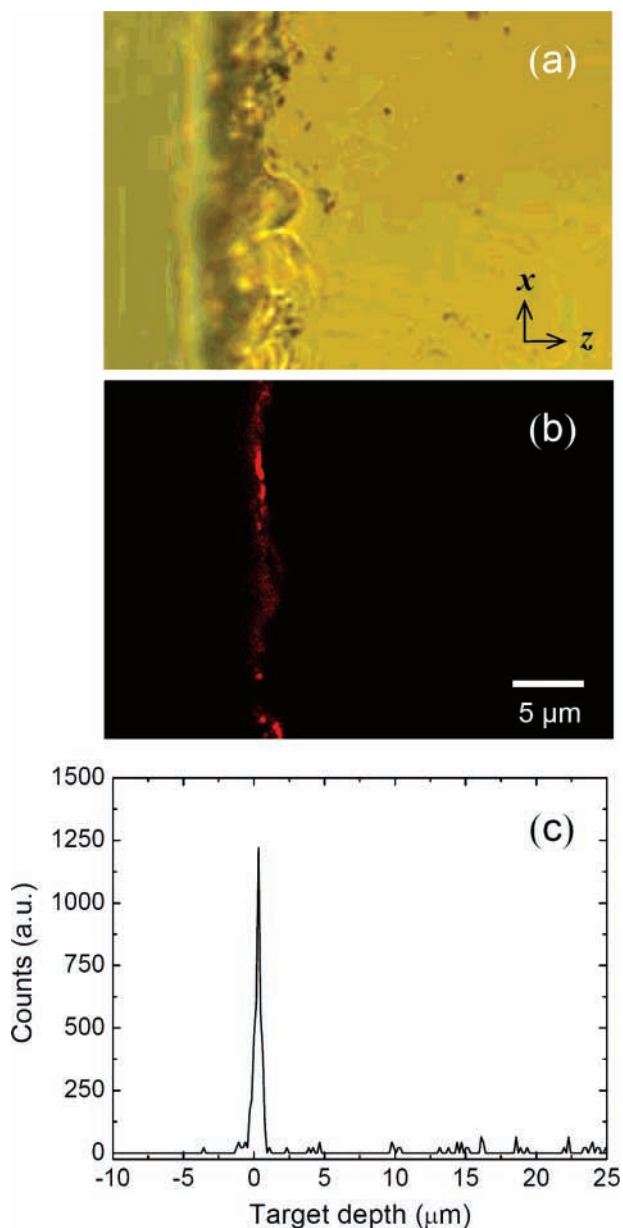
Figure 5. Characterization of a diamond substrate irradiated by 40 keV protons and annealed at 800 °C with confocal fluorescence microscopy; (a) bright field and (b) confocal fluorescence images of the substrate near one of its surface edges. A typical fluorescence intensity profile along the *z* axis is shown in (c).

bands,[32] quantitative understanding of the atomic nitrogen atoms and these centers in diamond has been possible. Figure 6a shows a typical infrared absorption spectrum of the as-received type Ib diamond single crystal in the defect-induced one-phonon region, that is, 900−1500 cm⁻¹. Two prominent features were observed at 1130 and 1344 cm⁻¹, and they have been attributed to the localized vibrational modes of C−N bonds in type Ib diamond.[33,34] The sharp peak at 1344 cm⁻¹ has a full-width at half-maximum (fwhm) of only 1.8 cm⁻¹, well suited for quantification purpose. On the basis of the relation derived by Lawson and co-workers[35]

$$[N^0] = 37.5\mu_{1344} \tag{2}$$

where $[N^0]$ is the concentration (in ppm) of atomic nitrogen in its neutral form and μ_{1344} is the absorption coefficient (in cm⁻¹) of the peak at 1344 cm⁻¹, we determined $[N^0] = 109 \pm 10$
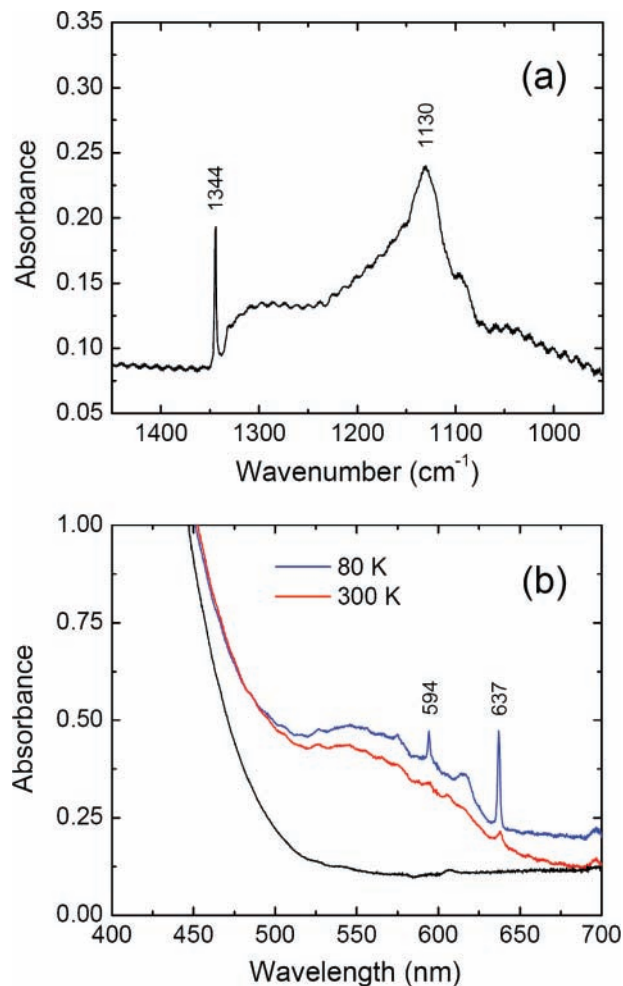

Figure 6. Spectroscopic characterization of type Ib diamond; (a) IR absorption spectrum of an as-received diamond single crystal and (b) UV−visible absorption spectra of the same crystal before (black curve) and after (red and blue curves) the proton irradiation and thermal annealing treatment. The UV−visible spectrum recorded at liquid nitrogen temperature is shifted vertically for clarity. The [100]-oriented diamond substrate used in this study has a thickness of 0.87 mm.

ppm. Alternatively, the nitrogen concentration can be determined from the absorption coefficient of the broader but more prominent feature at 1130 cm⁻¹ as[33,34]

$$[N^0] = (25 \pm 2)\mu_{1130} \tag{3}$$

In both cases (and also in relation 4 that follows), the absorption coefficient here is defined as $\mu = A/L \log e$, where A is the measured absorbance at the wavenumber of interest and L is the sample thickness (in cm).

Figure 6b shows a UV−visible OPA spectrum of the same sample characterized by IR spectroscopy in Figure 6a. No distinct feature was observed in the visible region, except for a smooth increase of the absorption starting at 550 nm due to the presence of isolated nitrogen atoms. The crystal became essentially opaque at the wavelength of $\lambda < 450$ nm, giving rise to an amber color. Exposure of the sample to the 3 MeV proton beam and subsequent annealing at 800 °C led to the emergence of a new absorption band centering at ∼560 nm with a fwhm of more than 100 nm. A zero-phonon line (ZPL) could be readily identified at 637 nm (1.945 eV), which is characteristic of the (N-V)⁻ center, and it sharpened up when the sample was cooled with liquid nitrogen. The width of this line decreased from 4.6 nm (or 14.2 meV) at room temperature to

2.0 nm (or 6.2 meV) at ~80 K. Similar to the previous study,[10] the ZPL of an unassigned nitrogen-related defect center could be found at 594 nm in the spectrum as well.

Observing the sharp ZPL at liquid nitrogen temperature offers a means to determine the $(N-V)^-$ concentration.[35,36] We calculated this concentration (centers/cm^3) based on the relation derived by Lawson et al.[35] and refined by Davies[32] as

$$[(N-V)^-] = (7.1 \pm 1.8) \times 10^{15} A_{637} \qquad (4)$$

where A_{637} (in meV·cm^{-1}) is the integrated absorption strength of the ZPL (637 nm or 1.945 eV) measured at ~80 K. In diamond, one ppm corresponds to 1.76×10^{17} atoms/cm^3. Taking $L = 50$ μm as derived from the confocal fluorescence measurement for the sample thickness, we determined a concentration of $[(N-V)^-] = 25 \pm 6$ ppm for the specimen irradiated by the 3 MeV protons at a dose of 1×10^{16} H$^+$/cm^2. This concentration suggests that in each cubic volume of 100 nm or 35 nm on a side, there exist 4400 or 190 $(N-V)^-$ defect centers in the crystal lattice, respectively. The latter is in line with our previous studies, indicating that a single 35 nm FND particle can contain up to 100 $(N-V)^-$ centers.[8] Assuming that these centers are uniformly distributed in the diamond lattice, the nearest neighbors are approximately separated by 5 nm.

It is of interest to compare our findings with the result of Lawson et al.[35] who used 1.9 MeV electrons for radiation damage of diamond. They estimated a concentration of 3.4 ppm for the $(N-V)^-$ centers produced by the electron irradiation at a dose of 2×10^{18} e$^-$/cm^2. In their experiment, 10 electrons produced 1 vacancy, and the subatomic particle penetrated ~2 mm of diamond. In contrast to the electron, a 3 MeV proton can produce ~13 vacancies when incident in the [100] direction (or ~10 vacancies in the [111] direction), although the penetration depth decreases to 50 μm.[26] Therefore, it would require a 100 times less dose of the protons to achieve the same vacancy concentration in the damaged region. The present experiment was conducted at a dose of 1×10^{16} H$^+$/cm^2, which is expected to produce 1.3×10^{17} vacancies/cm^2 (or 1.0×10^{17} vacancies/cm^2 in the [111] direction). Taking 50 μm as the effective sample thickness, we calculated that a vacancy concentration of 150 ppm (or 110 ppm in the [111] direction) resulted from the 3 MeV proton irradiation. This concentration is commensurate with the typical nitrogen concentration of the samples used in this experiment, and thus, overdosage was avoided. Compared to $[N^0] = 109$ ppm, our measurement of $[(N-V)^-] = 25$ ppm suggests that more than 23% of the N^0 atoms in the proton-damaged region had been converted to the $(N-V)^-$ centers after thermal annealing. This percentage compares favorably with the fraction of 0.30 as determined by Lawson et al.[35] in their experiments using 1.9 MeV electrons.[37] The agreement reflects the consistency between these two sets of measurements.

Containing more than 20 ppm of the $(N-V)^-$ centers, the proton-irradiated diamond substrate exhibits a discernible phonon sideband centering at ~560 nm above a continuous absorption background (Figure 6b). At room temperature, the ZPL appears only as a weak shoulder-like feature at 637 nm due to the thermal effect. Using $L = 50$ μm and $[(N-V)^-] = 25$ ppm, we determined an OPA cross section of $\sigma_{OPA} = (3.1 \pm 0.8) \times 10^{-17}$ cm^2 at 532 nm for this center. Note that this measured cross section is only about one-fifth that of rhodamine B in methanol.[38] However, the difference in the integrated absorption cross section between these two fluorophores is reduced to a factor of ~2 since the width of this absorption band is twice larger than that of rhodamine B at room
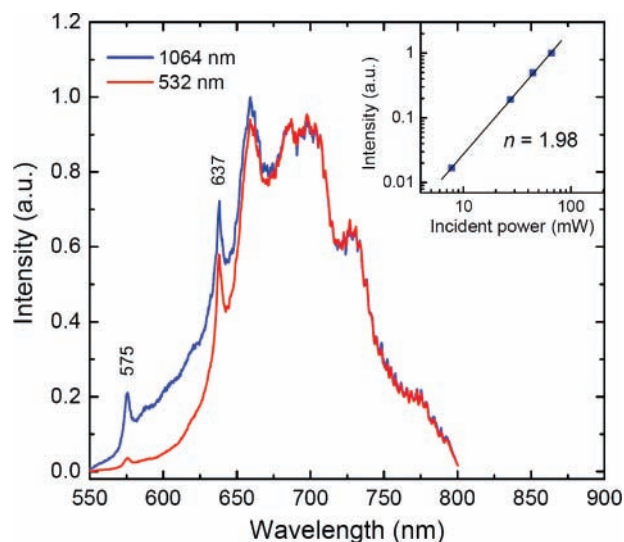

Figure 7. Comparison of one-photon and two-photon excited fluorescence spectra of nitrogen-vacancy centers in type Ib diamond treated with 3 MeV proton irradiation. Inset: Dependence of the fluorescence intensity on the incident energy of the 1064 nm excitation laser. Fitting the data to the relation $I \propto P^n$ shows a two-photon process.

temperature. The result is consistent with the fluorescence decay time measurements for the $(N-V)^-$ center, which shows a lifetime in the range of ~10 ns,[39,40] nearly twice longer than the ~4 ns of rhodamine B.

Two-Photon Fluorescence Spectra and Decay Lifetimes. Figure 7 displays the emission spectra of the $(N-V)^-$ centers excited by 532 and 1064 nm laser pulses at room temperature for a sample prepared with the 3 MeV proton irradiation. Both spectra were collected at an excitation time of 4 s using a 40× microscope objective with an incident laser power of 0.08 μW and 4.6 mW for the one-photon and two-photon excitations, respectively. In addition to the ZPL of the $(N-V)^-$ center at 637 nm, a sharp ZPL derived from the $(N-V)^0$ center can be found at 575 nm (2.156 eV) in both spectra. Interestingly, this center cannot be identified in the absorption spectrum even at 80 K (Figure 6b) but reveals itself clearly in the emission profile. The revelation of the $(N-V)^0$ center is more complete in the two-photon excitation, where a relatively more intensive ZPL band at 575 nm and its phonon sideband peaking at ~620 nm were detected.[41] Other than this marked difference, the one-photon and two-photon excited emission spectra are essentially identical, suggesting that the same states of the $(N-V)^-$ center are reached regardless of the mode of the excitation. Since it has been known that $(N-V)^0$ is the major contributor to the cathodoluminescence emitted by all diamonds,[41] the observation of this center in Figure 7 seems to imply that charge-transfer processes take place more efficiently during the two-photon excitation.

To confirm that the 1064 nm excitation is indeed a two-photon process, a power-dependence measurement of the fluorescence intensity yielded a slope of 1.98 ± 0.02 in the logarithmic plot (inset in Figure 7). No significant change in the fluorescence spectrum was observed over the intensity range of 1–13 GW/cm^2, and additionally, the difference in the fluorescence decay time between one-photon and two-photon excitations was within the limit of our experimental error, 6.3 ± 0.7 ns (Figure 8). It should be noted that the presently measured fluorescence decay lifetimes are substantially shorter than the literature value of 11.6 ns first reported by Collins et al.[39] for synthetic type Ib diamond. However, it is in closer agreement with the lifetime of 8.0 ns as recorded by Hanzawa et al.[40] for diamond substrates

(N-V)⁻ Centers in Proton-Irradiated Type Ib Diamond
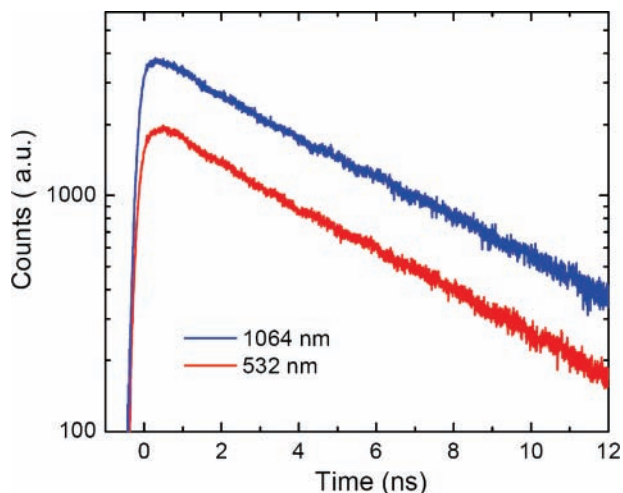
J. Phys. Chem. A, Vol. 111, No. 38, 2007 **9385**

Figure 8. Comparison of one-photon and two-photon excited fluorescence decays of nitrogen-vacancy centers in type Ib diamond treated with 3 MeV proton irradiation. Both decays have the same lifetime of 6.3 ± 0.7 ns.
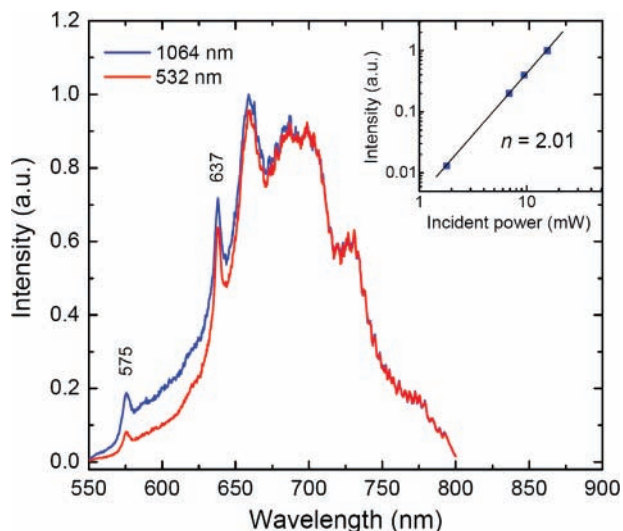

Figure 9. Comparison of one-photon and two-photon excited fluorescence spectra of nitrogen-vacancy centers in type Ib diamond treated with 40 keV proton irradiation. Inset: Dependence of the fluorescence intensity on the incident energy of the 1064 nm excitation laser. Fitting the data to the relation $I \propto P^n$ shows a two-photon process.

containing a high concentration (up to 50 ppm) of (N-V)⁻ defect centers produced by neutron irradiation and probed with a 20 ps laser.

Figure 9 shows the TPE spectra of a sample prepared with the 40 keV proton irradiation at room temperature. Both spectra were collected at an excitation time of 5 s using a 100× microscope objective with an incident laser power of 0.08 μW and 15.6 mW for one-photon and two-photon excitations, respectively. Time domain analysis of the fluorescence revealed that the (N-V)⁻ centers are photostable even under intensive excitation at a peak power density of 3 GW/cm² with the ps 1064 nm laser. The fluorescence intensity stayed essentially the same after several minutes of continuous excitation. From the power-dependence measurement over the intensity range of 0.3−3 GW/cm², a two-photon process with a slope of 2.01 ± 0.02 in the logarithmic plot was confirmed (inset in Figure 9). No significant change of the fluorescence spectrum was observed through different z-position scans. Of importance to remark here is that in this sample, the proton-beam-created N-V

centers were confined within a small region (∼0.23 μm thickness) near the diamond surface. Since the excitation laser was focused to a spot of ∼1 μm in diameter, the volume probed was estimated to be ∼2×10^8 nm³. This small volume suggests that we were equivalently probing ∼400 FND particles with a diameter of 100 nm in this experiment, given a volume of ∼5 $\times 10^5$ nm³ for the 100 nm sphere. Judging from the high signal-to-noise ratio of the dispersed fluorescence spectrum as shown in Figure 9, imaging of the individual 100 nm (or even 35 nm) FNDs isolated on a glass substrate or in a living cell with the two-photon fluorescence technique using a femtosecond laser is deemed practical.

Finally, in determining the two-photon absorption cross section of the (N-V)⁻ center, we first calibrated our optical systems against rhodamine B, whose one-photon and two-photon absorption cross sections have been well characterized.[19,20] To simulate the situation that the (N-V)⁻ centers are embedded in the diamond lattice and confined in a thin layer, the dye molecules were dispersed in a poly(methyl methacrylate) (PMMA) polymer matrix spin-coated on a microscope cover slide. The matrix so prepared had a thickness of ∼100 nm,[42] comparable to the thickness of the diamond sample treated with the 40 keV protons. Since both sample thicknesses were smaller than the focal depth (∼1 μm) of the microscope objective used in this experiment, complications arising from the use of a high NA objective could be avoided. For instance, aberrations due to the difference in refractive index between these two samples were minimized, and uniform illumination of the specimen along the vertical axis was ensured. To achieve high precision of this measurement, the vertical position of the microscope objective was carefully adjusted by a piezoelectric nanopositioner and kept at a site where the fluorescence intensity was maximal. A ratio of

$$\frac{\sigma_{\text{NV,TPA}}}{\sigma_{\text{NV,OPA}}} \bigg/ \frac{\sigma_{\text{RhB,TPA}}}{\sigma_{\text{RhB,OPA}}} = \left(\frac{I_{\text{NV,TPE}}}{I_{\text{NV,OPE}}}\right) \bigg/ \left(\frac{I_{\text{RhB,TPE}}}{I_{\text{RhB,OPE}}}\right) \times$$
$$\left(\frac{P_{\text{NV,532}}}{P_{\text{RhB,532}}}\right) \bigg/ \left(\frac{P_{\text{NV,1064}}}{P_{\text{RhB,1064}}}\right)^2 = 0.14$$

was obtained between TPE and OPE processes. Assuming that the absorption cross sections of rhodamine B dispersed in the PMMA matrix and in methanol solution are the same, that is, $\sigma_{\text{RhB,OPA}} = 1.4 \times 10^{-16}$ cm² at 532 nm and $\sigma_{\text{RhB,TPA}} = (14 \pm 7) \times 10^{-50}$ cm⁴·s/photon at 1064 nm,[20] we determined $\sigma_{\text{NV,TPA}} = (0.45 \pm 0.23) \times 10^{-50}$ cm⁴·s/photon based on the value of $\sigma_{\text{NV,OPA}} = (3.1 \pm 0.8) \times 10^{-17}$ cm² for the (N-V)⁻ center. Notably, this measured two-photon absorption cross section is about 30 times smaller than that of rhodamine B but is twice as large as that ($\sigma_{\text{TPA}} = 0.23 \times 10^{-50}$ cm⁴·s/photon) of fluorescein at 1050 nm.[19] Our previous experiment has shown that a single 35 nm FND can contain up to 100 (N-V)⁻ centers.[8] These particles (and smaller ones) can then compete with rhodamine B (and other dye molecules) in terms of their TPA cross sections.

Conclusions

The interaction of protons with type Ib bulk diamond has been investigated with IR/UV−visible absorption spectroscopies and confocal fluorescence microscopy. The investigation was motivated by the development of an economic method for production of high-brightness FNDs using a medium-energy proton beam for wide biological applications. This work demonstrates that a (N-V)⁻ concentration of more than 10 ppm

can be readily achieved by exposing a diamond single crystal to 40 keV protons at a dose of 6×10^{14} H$^+$/cm^2. It leads to the suggestion that each type Ib diamond nanocrystallite of a size of 35 nm can contain up to 100 photostable (N-V)$^-$ centers if they are treated under the same conditions. We anticipate that after proper selection of the ion sources, optimization of the beam irradiation conditions, and increase of the nitrogen contents, the fluorescence brightness of the individual FNDs can be further enhanced by 1 order of magnitude.

When using FND as an optical probe, it is desirable to take advantage of two-photon fluorescence microscopy, which has opened up many new possibilities for biomedical imaging and diagnosis.[15] Ultrafast lasers operating in the near-infrared ($\sim$1 μm) region are well suited for this purpose. We have systematically measured in this work both the one-photon and two-photon absorption cross sections of the (N-V)$^-$ centers in type Ib diamond to be $\sigma_{OPA} = 3.1 \times 10^{-17}$ cm^2 at 532 nm and $\sigma_{TPA} = 0.45 \times 10^{-50}$ cm$^4 \cdot$s/photon at 1064 nm. While the latter is $\sim$30 times smaller than that of rhodamine B, the deficit can be easily compensated by using particles containing multiple defect centers. The present study, focused on the nonlinear photophysical properties of the (N-V)$^-$ centers in bulk diamond, has lent promise to the two-photon fluorescence imaging and tracking of the individual FNDs in living cells. Further improvement of the sensitivity of this method, conceivably by more than 3 orders of magnitude, can be achieved with the use of femtosecond lasers. Such experiments are currently being performed in our laboratories.

References and Notes

(1) Yang, W. S.; Auciello, O.; Butler, J. E.; Cai, W.; Carlisle, J. A.; Gerbi, J.; Gruen, D. M.; Knickerbocker, T.; Lasseter, T. L.; Russel, J. N.; Smith, L. M.; Hamers, R. J. *Nat. Mater.* **2002**, *1*, 253.

(2) Hartl, A.; Schmich, E.; Garrido, J. A.; Hernando, J.; Catharino, S. C. R.; Walter, S.; Feulner, P.; Kromka, A.; Steinmuller, D.; Stutzmann, M. *Nat. Mater.* **2004**, *3*, 736.

(3) Kruger, A. *Angew. Chem., Int. Ed.* **2006**, *45*, 6426.

(4) Yu, S.-J.; Kang, M.-W.; Chang, H.-C.; Chen, K.-M.; Yu, Y.-C. *J. Am. Chem. Soc.* **2005**, *127*, 17604.

(5) Schrand, A. M.; Huang, H. J.; Carlson, C.; Schlager, J. J.; Osawa, E.; Hussain, S. M.; Dai, L. M. *J. Phys. Chem. B* **2007**, *111*, 2.

(6) (a) Huang, L.-C. L.; Chang, H.-C. *Langmuir* **2004**, *20*, 5879. (b) Kong, X. L.; Huang, L.-C. L.; Hsu, C.-M.; Chen, W.-H.; Han, C.-C.; Chang, H.-C. *Anal. Chem.* **2005**, *77*, 259. (c) Kong, X. L.; Huang, L.-C. L.; Liau, S.-C. V.; Han, C.-C.; Chang, H.-C. *Anal. Chem.* **2005**, *77*, 4273. (d) Chen, W.-H.; Lee, S.-C.; Sabu, S.; Fang, H.-C.; Chung, S.-C.; Han, C.-C.; Chang, H.-C. *Anal. Chem.* **2006**, *78*, 4228. (e) Ngyuen, T.-T.-B.; Chang, H.-C.; Wu, V. V. W.-K. *Diamond Relat. Mater.* **2007**, *16*, 872.

(7) Kruger, A.; Liang, Y. J.; Jarre, G.; Stegk, J. *J. Mater. Chem.* **2006**, *16*, 2322.

(8) Fu, C.-C.; Lee, H.-Y.; Chen, K.; Lim, T.-S.; Wu, H.-Y.; Lin, P.-K.; Wei, P.-K.; Tsao, P.-H.; Chang, H.-C.; Fann, W. *Proc. Natl. Acad. Sci. U.S.A.* **2007**, *104*, 727.

(9) Clark, C. D.; Norris, C. A. *J. Phys. C: Solid State Phys.* **1971**, *4*, 2223.

(10) Davies, G.; Hamer, M. F. *Proc. R. Soc. London, Ser. A* **1976**, *348*, 285.

(11) Mita, Y. *Phys. Rev. B* **1996**, *53*, 11360.

(12) (a) Jelezko, F.; Tietz, C.; Gruber, A.; Popa, I.; Nizovtsev, A.; Kilin, S.; Wrachtrup, J. *Single Mol.* **2001**, *2*, 255. (b) Jelezko, F.; Wrachtrup, J. *Phys. Status Solidi A* **2006**, *203*, 3207.

(13) Lim, Y. T.; Kim, S.; Nakayama, A.; Stott, N. E.; Bawendi, M. G.; Frangioni, J. V. *Mol. Imaging* **2003**, *2*, 50.

(14) Denk, W.; Strickler, J. H.; Webb, W. W. *Science* **1990**, *248*, 73.

(15) Xu, C.; Zipfel, W.; Shear, J. B.; Williams, R. M.; Webb, W. W. *Proc. Natl. Acad. Sci. U.S.A.* **1996**, *93*, 10763.

(16) Helmchen, F.; Denk, W. *Nat. Methods* **2005**, *2*, 932.

(17) Göppert-Mayer, M. *Ann. Phys.* **1931**, *9*, 273.

(18) Shen, Y. R. *The Principles of Nonlinear Optics*; New York: Wiley, 1984; p 202.

(19) Xu, C.; Webb, W. W. *J. Opt. Soc. Am. B* **1996**, *13*, 481.

(20) Hermann, J. P.; Ducuing, J. *Opt. Commun.* **1972**, *6*, 101.

(21) Edwards, D. F.; Philipp, H. R. In *Handbook of Optical Constants of Solids*; Palik, E. D., Ed.; Academic: Orlando, FL, 1985; p 665.

(22) (a) Meijer, J.; Burchard, B.; Domhan, M.; Wittmann, C.; Gaebel, T.; Popa, I.; Jelezko, F.; Wrachtrup, J. *Appl. Phys. Lett.* **2005**, *87*, 261909. (b) Rabeau, J. R.; Reichart, P.; Tamanyan, G.; Jamieson, D. N.; Prawer, S.; Jelezko, F.; Gaebel, T.; Popa, I.; Domhan, M.; Wrachtrup, J. *Appl. Phys. Lett.* **2006**, *88*, 023113.

(23) Bourgoin, J. C.; Massarani, B. *Phys. Rev. B* **1976**, *14*, 3690.

(24) Koike, J.; Parkin, D. M.; Mitchell, T. E. *Appl. Phys. Lett.* **1992**, *60*, 1450.

(25) Ziegler, J. F.; Biersack, J. P.; Littmark, U. *The Stopping and Range of Ions in Solids*; Pergamon: New York, 1985. Free SRIM software is available from the website, http://www.srim.org/

(26) A penetration depth of $\sim$50 μm was also predicted by the SRIM simulation for the 3 MeV protons incident in the [111] direction of type Ib diamond substrates, although the number of vacancies produced per proton was reduced from 13 to 10 because of the increase of the displacement energy from 37.5 to 45 eV (ref 24).

(27) Prins, J. F. *Semicond. Sci. Technol.* **2003**, *18*, S27.

(28) Kalish, R. In *Properties and Growth of Diamond*; Davies, G., Ed.; EMIS Datareviews Series No. 9; INSPEC, The Institute of Electrical Engineers: London, 1994; Chapter 6.4, p 196.

(29) Brunetto, R.; Baratta, G. A.; Strazzulla, G. *J. Appl. Phys.* **2004**, *96*, 380.

(30) Newton, R. L.; Davidson, J. L.; Lance, M. J. *Diamond Relat. Mater.* **2005**, *14*, 173.

(31) Gruber, A.; Dräbenstedt, A.; Tietz, C.; Fleury, L.; Wrachtrup, J.; von Borczyskowski, C. *Science* **1997**, *276*, 2012.

(32) Davies, *Physica B* **1999**, *273−274*, 15.

(33) Woods, G. S.; van Wyk, J. A.; Collins, A. T. *Philos. Mag.* **1990**, *62*, 589.

(34) Kiflawi, I.; Mayer, A. E.; Spear, P. M.; van Wyk, J. A.; Woods, G. S. *Philos. Mag. B* **1994**, *69*, 1141.

(35) Lawson, S. C.; Fisher, D.; Hunt, D. C.; Newton, M. *J. Phys.: Condens. Matter* **1998**, *10*, 6171.

(36) Davies, G.; Lawson, S. C.; Collins, A. T.; Mainwood, A.; Sharp, S. J. *Phys. Rev. B* **1992**, *46*, 13157.

(37) The fraction 0.30 was recalculated by using relation 4 in text and the experimental data given in ref 35.

(38) Birge, R. R. *Kodak Laser Dyes*; Eastman Kodak Company: Rochester, NY, 1987.

(39) Collins, A. T.; Thomaz, M. F.; Jorge, M. I. B. *J. Phys. C: Solid State Phys.* **1983**, *16*, 2177.

(40) Hanzawa, H.; Nisida, Y.; Kato, T. *Diamond Relat. Mater.* **1997**, *6*, 1595.

(41) Davies, G. *J. Phys. C: Solid State Phys.* **1979**, *12*, 2551.

(42) Hall, D. B.; Underhill, P.; Torkelson, J. M. *Polym. Eng. Sci.* **1998**, *38*, 2039.